Electronic Supplementary Material (ESI) for ChemComm.

Supporting Information

An Ion Signal Responsive Dynamic Protein Nano-spring Constructed by High Ordered Host-Guest Recognition

Chengye Si,[a †] Jiaxi Li,[a †] Quan Luo,[a] Chunxi Hou,[a] Tiezheng Pan,[a] Hongbin Li,[b] and Junqiu Liu[a]*

[a] State Key Laboratory of Supramolecular Structure and Materials, College of Chemistry, Jilin University, 2699 Qianjin Street, Changchun 130012, China, Fax: (+86) 0431-85168452

[b] Department of Chemistry, University of British Columbia Vancouver, British Columbia, Canada V6T 1Z1.

† C. Y. Si and J. X. Li contributed equally to this work.

*Email: junqiuliu@jlu.edu.cn

Contents

1. Construction of the plasmid encoding for fusion protein FGG-recoverin-GST

Our construction strategy was shown in Figure S1. First, recoverin open reading frame was amplified with the template pET-11a using the primers recoverin-a (R-a, 5'-CCCATATGTTTGGAGGAGGGAACAGCAAGAGTGG-3') and Linker-b (L-b, 5'-CCAATAACCTAGTATAGGGGAGAGTTTCTTTTCCTTCAGTTT-3'). The underline sequence was the recognition site for restriction endonuclease Nde I, and the bold sequence was tripeptide FGG-encoding sequence. The GST open reading frame was amplified with the template pGEX-5X-2 using the primers Linker-a (L-a, 5'-TCCCCTATACTAGGTTATTGG-3') and GST-b (G-b, 5'-CCGCTCGAGTTATTTTGGAGGATGGTCG-3'). The underline sequence in G-b was the recognition site for restriction endonuclease Xho I. Part sequence of L-b which was marked by red was designed to complement the whole sequence of L-a. The purified PCR fragments of the sequences of both recoverin and GST were joint together in the third step, as these two DNA fragments complemented to each other. Primers R-a and G-b can be used together in this step as their anneal temperature were also closed. After the PCR reaction, the main band of the PRC productions was collected by gel extraction. Next the FGG-recoverin-GST fragments and plasmid pET-22b were digested with the restriction endonucleases Nde I and Xho I. At last, purified inserts of the sequence of fusion protein FGG-recoverin-GST and plasmid pET-22b were recombined by T4 DNA ligase.

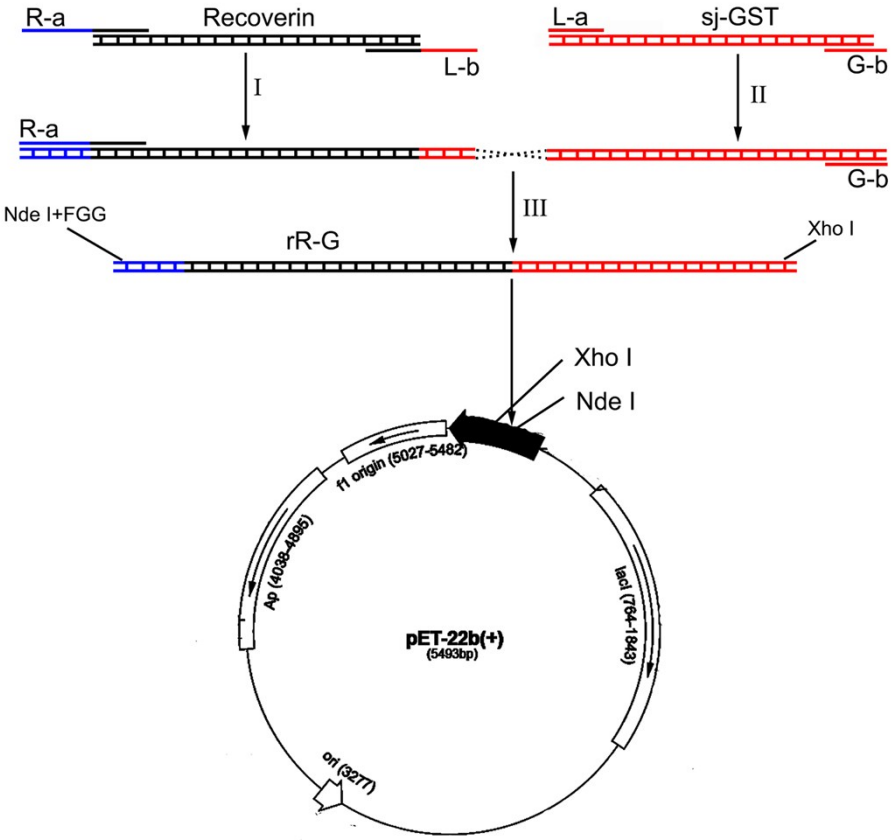

Figure S1. Construction of the expression plasmid (pET-22b) of fusion protein FGG-recoverin-GST.

1.1 Agarose gel electrophoresis (AGE) analysis of PCR products of sj-GST and FGG-recoverin

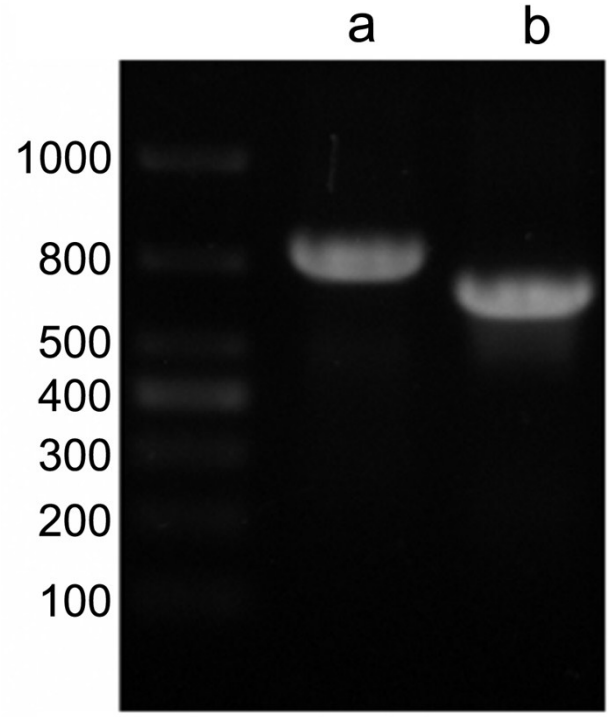

Figure S2. Agarose gel electrophoresis analysis. a) PCR products of sj-GST. b) PCR products of FGG-recoverin. The agarose percentage of the AGE gels is 1%.

1.2 Agarose gel electrophoresis (AGE) analysis of recombinant plasmid of FGG-recoverin-GST (pET-22b)

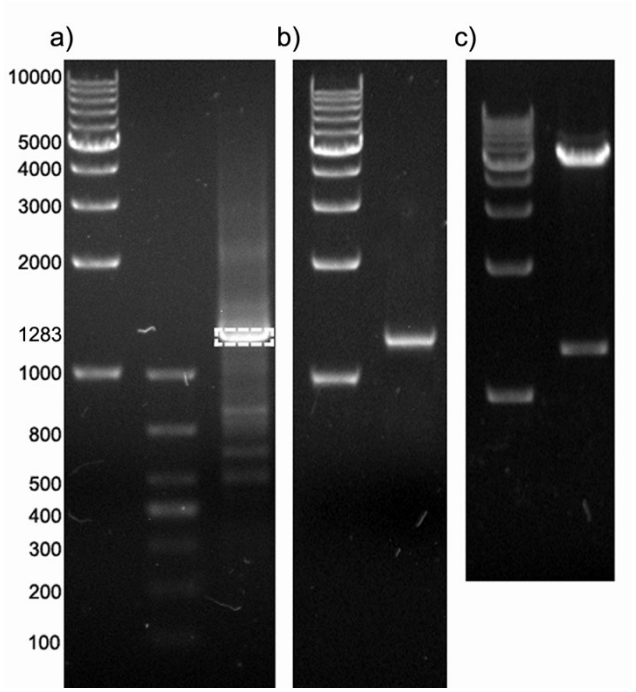

Figure S3. Agarose gel electrophoresis analysis. a) PCR products of FGG-recoverin-GST. b) Gel extraction products of FGG-recoverin-GST. c) Dual-enzyme digestion of FGG-recoverin-GST (pET-22b). The agarose percentage of the AGE gels is 1%.FGG-recoverin-GST (pET-22b). The agarose percentage of the AGE gels is 1%.

1.3 Protein Sequences

The sequences of fusion protein FGG-recoverin-GST are listed below. The red part is FGG-tag of the fusion protein. The blue part is recoverin domain of the fusion protein. The green part is sj-GST domain of the fusion protein.

MFGGGNSKSGALSKEILEELQLNTKFTEEELSSWYQSFLKECPSGRITRQEFQTIYSK FFPEADPKAYAQHVFRSFDANSDGTLDFKEYVIALHMTSAGKTNQKLEWAFSLYDV DGNGTISKNEVLEIVTAIFKMISPEDTKHLPEDENTPEKRAEKIWGFFGKKDDDKLT EKEFIEGTLANKEILRLIQFEPQKVKEKLKEKKLSPILCYWKIKGLVQPTRLLLEYLE EKYEEHLYERDEGDKWRNKKFELGLEFPNLPYYIDGDVKLTQSMAIIRYIADKHNM LGGSPKERAEISMLEGAVLDIRYGVSRIAYSKDFETLKVDFLSKLPEMLKMFEDRLC HKTYLNGDHVTHPDFMLYDALDVVLYMDPMCLDAFPKLVSFKKRIEAIPQIDKYLK SSKYIAWPLQGWQATFGGGDHPPK

2. Over expression and purification of fusion protein FGG-recoverin-GST

The construction of FGG-recoverin-GST plasmid was described in Figure S1. The constructed plasmid was transformed into *Escherichia Coli* BL21 (DE3). The expression stain grew in 1L LB liquid medium with 100mg/L Amp witch was placed in the 37℃ shaking incubator. When the OD600 value reach 0.6, 0.5mM IPTG was added to induce the expression. After cultured for 20 hours, the cells were collected and sonic disrupted with 50nM phosphate buffered saline (PBS, pH=7.4, containing 1mM PMSF). The cell homogenates was centrifuged under 4°C at 15000rpm for 30min. The supernatant was loaded in a pretreated glutathione affinity column and kept cyclic loading under 4℃ overnight. The impurity proteins were washed off by 50mM PBS buffer (pH=7.4), then the target protein was eluted with 50mM Tris-HCl buffer containing 10mM reduced glutathione (pH=8.0). The eluent was dialyzed by 8kDa cut off dialysis membrane to ultrapure water. At last the sample was lyophilized to dry powder for the next experiments. The desired proteins were confirmed through SDS-PAGE analysis, CD spectra and matrix-assisted laser desorption/ ionization time of flight mass spectrometry (MALDI-TOF) analysis.

2.1 SDS-PAGE analysis of fusion protein FGG-recoverin-GST

Lane 1: Protein Marker. Lane 2: *E.coli BL21* (DE3) containing fusion protein FGG-recoverin-GST vector (pET-22b) without isopropyl-β-d-thiogalactopyranoside (IPTG) induction; Lane 3: BL21 (DE3) containing fusion protein FGG-recoverin-GST vector (pET-22b) with 0.5 mM IPTG induction; Lane 4: purified fusion protein FGG-recoverin-GST from the glutathione Sepharose. The acrylamide percentage of the SDS-PAGE gels is 15%.

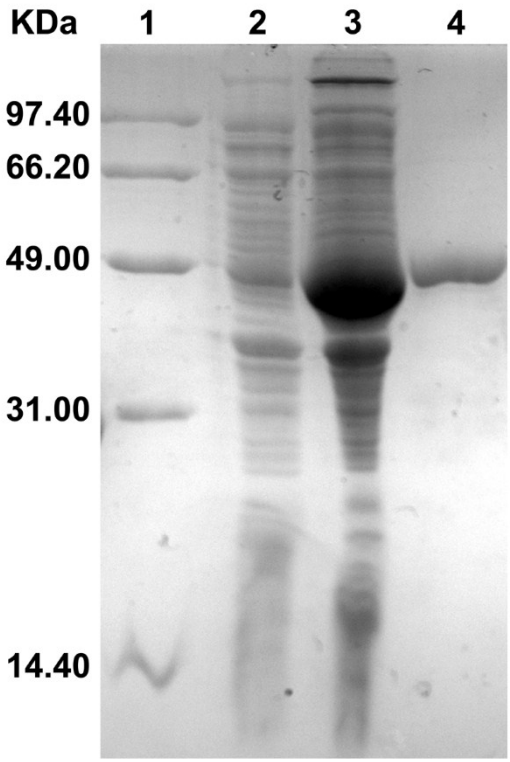

Figure S4. SDS-PAGE polyacrylamide gel electrophoresis.

2.2 CD spectra of fusion protein FGG-recoverin-GST

Measurements of CD spectra were performed using a MOS-450/AF-CD spectropolarimeter (Bio-Logic, France) equipped with a thermostated cell holder, using a 0.1 cm quartz cell. Spectra were collected by averaging three scans using protein at a concentration of 1μM for Ca^{2+}-free and Ca^{2+}-binding FGG-recoverin-GST.

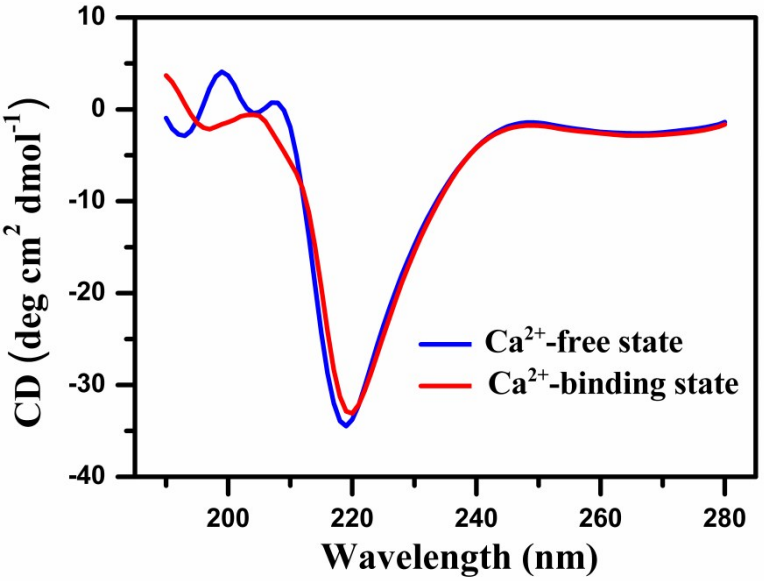

Figure S5. CD spectra of fusion protein FGG-recoverin-GST.

2.3 MALDI TOF mass spectra of fusion protein FGG-recoverin-GST.

MALDI-TOF mass spectrometry was performed using autoflex speedTM TOF/TOF mass spectrometer (Bruker, daltonics Inc., USA). The protein sample was desalted by dialysis against ultrapure water with dialyzing tubes, Slide-A-Lyzer Dialysis Cassettes (Pierce) or G25 filtration. The resulting GST derivatives were lyophilized and resolved at a concentration of 10 μM. For preparation, sinapic acid was chosen as matrix which was saturated in 70% acetonitrile and supplemented with 1‰ trifluoroacetic acid. 1μL samples and 1μL matrix were sequentially dropped onto the ground steel and dried in air.

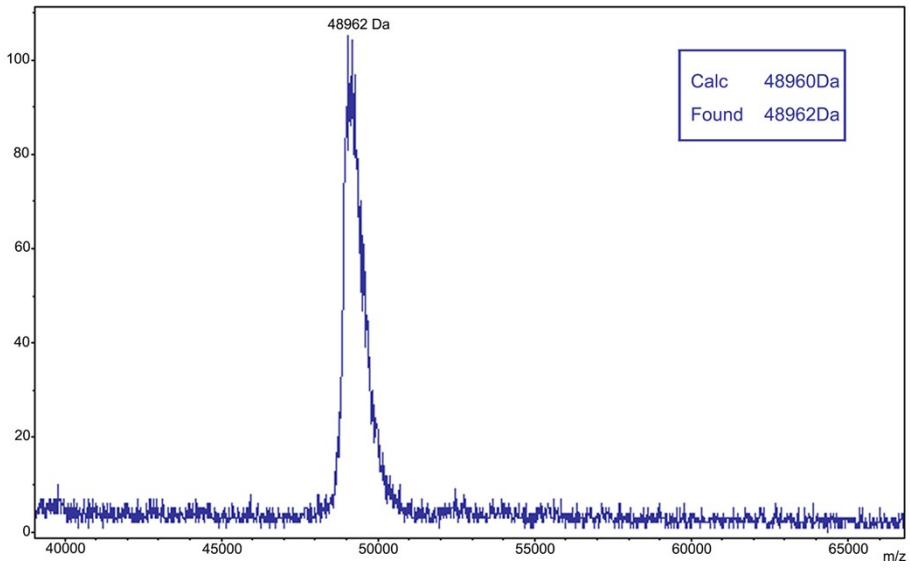

Figure S6. MODI-TOF mass spectra of fusion protein FGG-recoverin-GST.

3. Size exclusion HPLC measurement of assemblies formed by fusion protein FGG-recoverin-GST and CB[8]

The assemblies formed by fusion protein FGG-recoverin-GST and CB[8] was first examined by size exclusion HPLC (Figure S7). The concentration of fusion protein FGG-recoverin-GST was fixed to 0.1μM. The retention time of fusion protein FGG-recoverin-GST was 13min and FGG-recoverin-GST dimer was 11min. The addition of CB[8] to FGG-recoverin-GST solution at the ratio of 1:2 resulted in a new peak with a retention time of 4min which was close to the death time of HPLC. Size exclusion HPLC result indicated the formation of large protein assemblies.

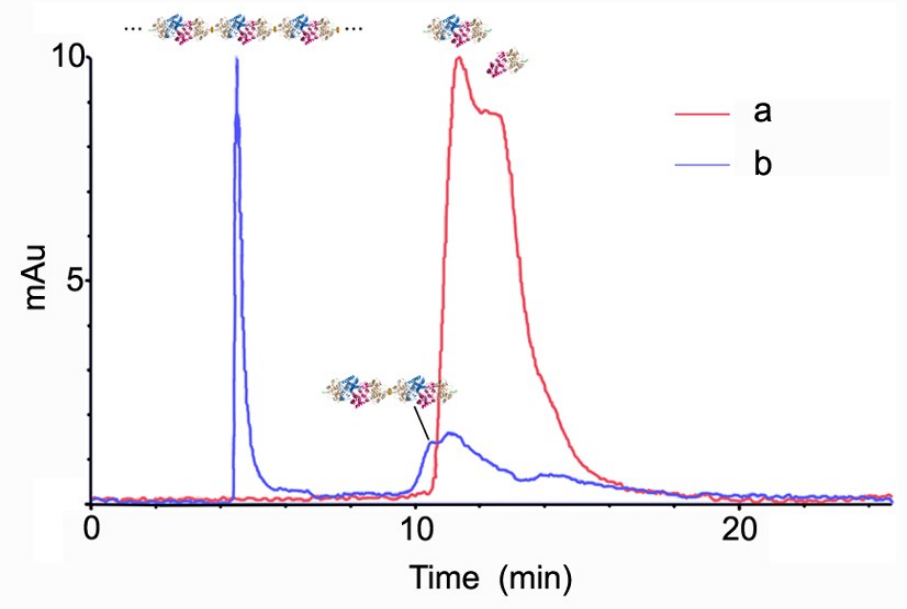

Figure S7. Size exclusion HPLC of protein assemblies. a) 0.1μM fusion protein FGG-recoverin-GST solution; b) The mixture of 0.1μM fusion protein FGG-recoverin-GST and 0.2μM of CB[8].

4. Dynamic light scattering (DLS) analysis of assemblies formed by fusion protein FGG-recoverin-GST and CB[8]

After using size exclusion HPLC to confirm the formation of protein assemblies, DLS was forward used to measure the average size of the protein assemblies (Figure S8). The concentration of fusion protein FGG-recoverin-GST was fixed to 5μM. The average size of fusion protein FGG-recoverin-GST was about 7.5nm which was identified with computer simulation result. After adding CB[8] to FGG-recoverin-GST solution at the ratio of 1:2 the average size changed to more than 300nm. DLS results also gave strong evidence of the formation of nano scale protein assemblies.

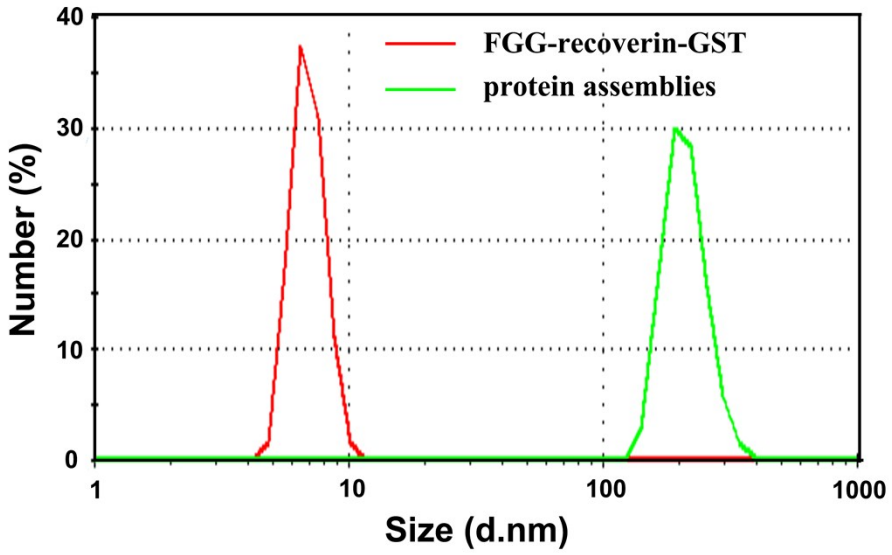

Figure S8. Dynamic light scattering (DLS) analysis of fusion protein FGG-recoverin-GST and protein assemblies.

5. Atomic force microscope (AFM) analysis of protein nanowires at a relative high protein concentration

When the concentrations of fusion protein FGG-recoverin-GST and CB[8] increased to 5μM and 2.5μM respectively, a large number of uniformly distributed nanowires were observed in the AFM image (Figure 1e, f). The height of double times of fusion protein FGG-recoverin-GST was observed at the crossover of nanowires in associated height profile images (Figure S9). This result indicated that some of these nanowires began to cover each other at this concentration. However, further aggregations like nanowire bundles or planar network have not been observed. This was because C2-symmetric FGG-recoverin-GST dimer was design to assemble in the symmetric axis orientation. Herein, the increase of concentration can only lead to a growth of the length of nanowires, but cannot lead to a further crosslinking.

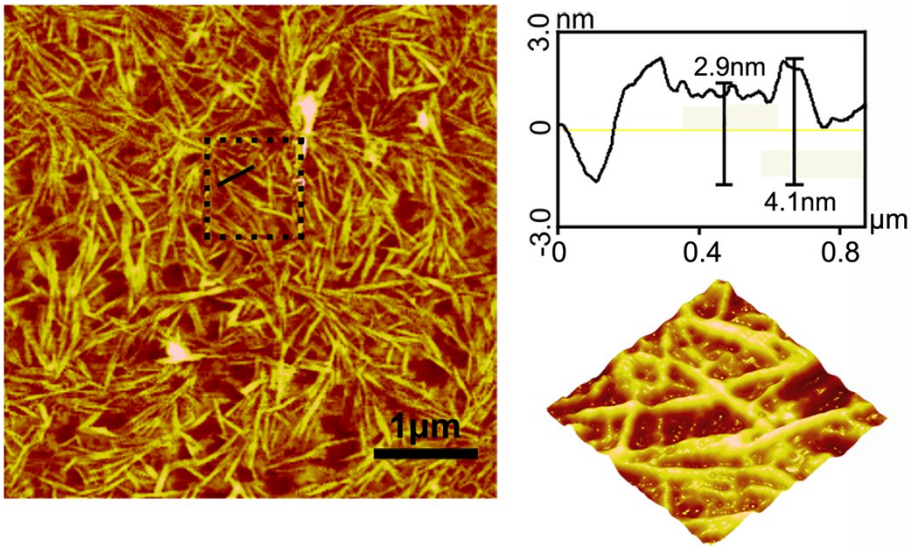

Figure S9. AFM analysis of protein nanowires at a relative high protein concentration.

6. Schematic representations of structure change of fusion protein FGG-recoverin-GST between binding and unbinding of Ca^{2+}

The addition of Ca^{2+} resulted in an exposure of flexible chain from recoverin domain of FGG-recoverin-GST (Figure S10a). By this way, the length of every building block of protein nanowires changed from 10.4nm to 15.5nm (Figure S10b), leading to longer and more stretch protein assembled nanostructures. The extended state of the assemblies can be as much as 50% longer than the contracted state theoretically.

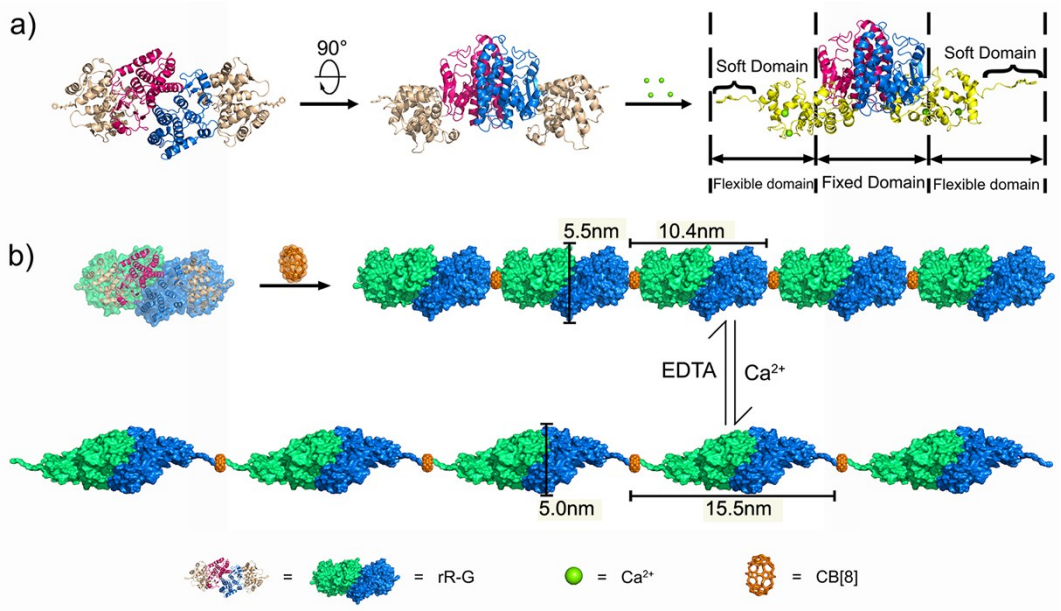

Figure S10. Schematic representations of a) detailed secondary structure change of fusion protein FGG-recoverin-GST after the binding of Ca^{2+} and b) structure change of each building block of nano-spring between binding and unbinding of Ca^{2+}.

7. Dynamic light scattering (DLS) analysis of fusion protein FGG-recoverin-GST at different states

The fusion protein FGG-recoverin-GST has a response of Ca^{2+} which is benefit from the recoverin domain. FGG-recoverin-GST was at contracted state without Ca^{2+}. At this time, the average size of fusion protein FGG-recoverin-GST was 7.5nm (Figure S11). FGG-recoverin-GST was at extended state after sufficient binding with Ca^{2+}. DLS result showed that the average size of fusion protein FGG-recoverin-GST was 12.7nm under extended state which had an obvious increase compared to contracted state. The microscopic change of size in each building block of protein nano-spring formed by fusion protein FGG-recoverin-GST resulted in a macroscopic observable change of size in nanostructures.

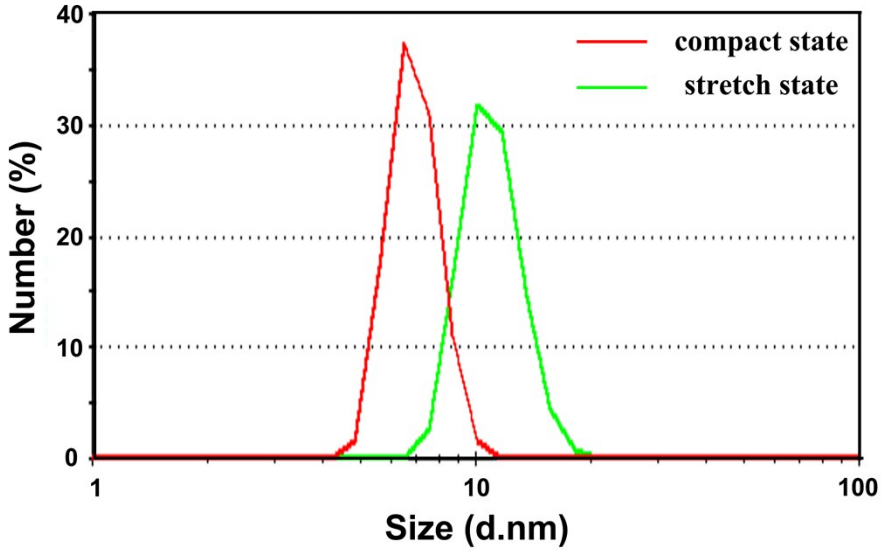

Figure S11. Dynamic light scattering (DLS) analysis of fusion protein FGG-recoverin-GST at different states.

8. Atomic force microscope (AFM) analysis of the extended state (state II) of protein nano-spring

The exposure of flexible chain from fusion protein FGG-recoverin-GST under state II lead to the linker of each building block of nano-spring changed from relative rigid to flexible. Therefore, the nano-spring showed slightly free radians under state II. However, the flexible linker resulted in the arrangement of different building blocks of nano-spring happened not always in the same direction. Herein, there were even some nanowires bending to two directions under state II (Figure S12)

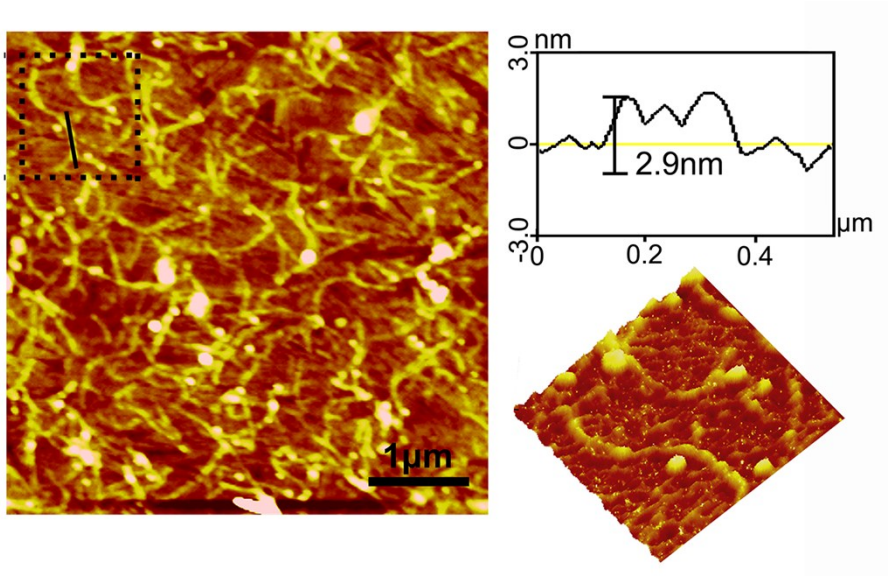

Figure S12. AFM) analysis of the extended state (state II) of protein nano-spring.

9. Transmission electron microscopy (TEM) analysis of the protein nano-spring

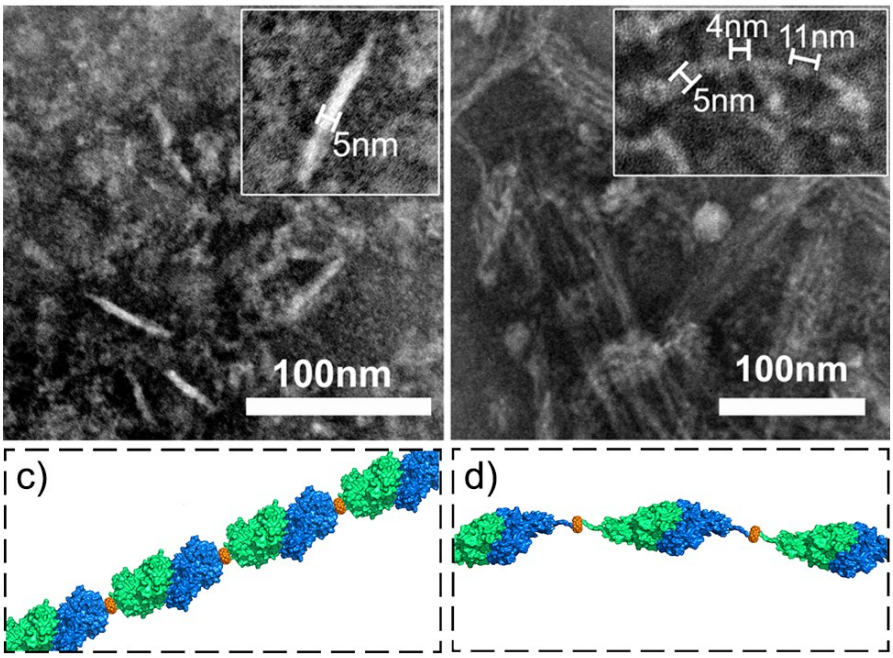

Figure S13. TEM images of a) contracted state and b) extended state of protein nano-spring. Schematic representations of c) contracted state and d) extended state of protein nano-spring.